We are IntechOpen, the world's leading publisher of Open Access books Built by scientists, for scientists

4,800
Open access books available

122,000
International authors and editors

135M
Downloads

Our authors are among the

154
Countries delivered to

TOP 1%
most cited scientists

12.2%
Contributors from top 500 universities

CLARIVATE ANALYTICS BOOK CITATION INDEX INDEXED

WEB OF SCIENCE™

Selection of our books indexed in the Book Citation Index in Web of Science™ Core Collection (BKCI)

Interested in publishing with us?
Contact book.department@intechopen.com

Numbers displayed above are based on latest data collected.
For more information visit www.intechopen.com

26

Objects Localization and Differentiation Using Ultrasonic Sensors

Bogdan Kreczmer
The Institute of Computer Engineering, Control and Robotics, University of Technology
Poland

1. Introduction

The most crucial problem for the mobile robot navigation is obstacles detection and their localization. The determination of obstacle position should be as accurate as possible in order to support robot self-localization procedures. In order to increase its efficiency the recognition of some feature of obstacles shapes should be done.
The most advanced systems use laser range-finder and vision to solve this task. They allow to obtain a lot of data of a robot environment and the delivered information is quite precise. Unfortunately these devices have some important drawbacks. Laser scanning range-finders are still expensive. Their another drawback is that they scan only in a single plain. It causes that some obstacle cannot be detected. There are also available 3D laser range-finders. But measurements performed by them are time consuming. Therefore it is rather difficult to use them for on-line mobile robot navigation when a robot moves during a measurement execution. Considering vision systems the main disadvantages are computation consuming methods and a price of the system.
In this sense ultrasonic range-finders seems still to be very useful equipment for a mobile robot. Their important advantage is low price and simplicity. Considering robotics applications they seem to be very attractive comparing especially with laser range-finders and vision systems. But in current mobile robots the ultrasonic sensors are rather used as an auxiliary equipment allowing to obtain rough information of the environment. The main reason of this situation is that the obtained data from commercial ultrasonic range-finders are very difficult to interprete. In this chapter two methods are presented which makes possible to overcome some difficulties combined with ultrasonic sensing. The first one is dedicated to the problem of object differentiation. The second method addresses the problem of an object localization and simplification of necessary computations.

2. Ultrasonic sensing

The result of a measurement performed by a commercial ultrasonic range-finder is time of flight (TOF) during which an ultrasonic signal is propagated from a sender to an obstacle and, after being reflected, back to a receiver. This is enough to compute the distance of the

path. In this way the form of the data obtained form sonars is very simple. Unfortunately this type of information is not easy to interpret. The main reason of their disadvantage is a wide beam of an emitted signal ($20^\circ \sim 50^\circ$). Traditional range-finder contains a single sender and a single receiver or a transducer which can work as a sender and than as a receiver. The wide emitted beam causes that they suffer from a very pure resolution. This type of beam smears the location of the object reflecting an echo and produces arcs when a rotational scan of the environment is performed. The extent of the arcs is related to the reflecting strength of the object Kuc & Siegel, (1987)Leonard & Durrant-Whyte, (1991)Kleeman & Kuc, (1995). In this case, the distance information that sonars provide is fairly accurate in depth, but not in an angle.

Another reason is combined with a frequency of an emitted wave packet. Because the frequency is usually $40kHz$ (piezo electric transducers) or $50kHz$ (electrostatic transducers) the length of the wave in air is about $8.5mm$ and $6.8mm$ respectively. When irregularities of an object surface are much smaller than the wave length of an ultrasonic signal then the surface can be treated as a kind of an acoustic mirror. Thus many objects in indoor environments can be assumed to be specular reflectors for ultrasonic waves. It causes that sometimes a sonar receives a multi-reflected echo instead of the first one. These reflections produce artifacts which are a false image of no existing object behind a real one or sometimes even in front of it. This last phenomena can be observed when several successive measurement are performed in regular short intervals. In this case it can happen that instead of receiving echo caused by a current emitted signal an echo produced by previous emission is detected. Considering cases of false images created by double reflections the well know example is a room corner. While a single sonar scanner is used, it isn't possible to distinguish it from a single wall because the same sequence of echos is obtained.

Using a single sonar it isn't possible correctly to distinguish the case of a single and multi-reflection. The picturesque description of the problem has been presented in Brown, (1985). Brown compared sensing with ultrasonics to trying to navigate in a house of mirrors using only a flash light. This is true if rooms, through which the robot navigates, contain only plain walls (in relation to the length of ultrasonic wave). Fortunately in indoor environment there are a lot of objects which are the source of direct echos. It means signals which are reflected by a single object and then detected by a sonar. But it doesn't help very much when a scanning range-finder consisting of a single sonar is used. Obtained data cannot be properly interpreted because it doesn't exist well defined one-to-one mapping between a contour of ultrasonic distance map and surfaces of objects or objects them self. In spite of that ultrasonic sensing has an immense potential to mobile robot navigation. In the animal world the well known examples of successful usage of ultrasonic waves for navigation are bats and dolphins. They can properly navigate in a very difficult conditions. For example small bats are able to fly at full speed through wire grid structures that are only slightly larger than their wingspan Cheeke, (2002). The main difference between a scanning ultrasonic range-finder and a bat is that the bat has two ears. They allow the bat to determine direction from which echo comes. In addition it was shown in Schillebeeckx et al., (2008) that a pinna can significantly influence on directivity pattern of a receiver which can be helpful for localization purposes.

But even using a single sonar it is possible to increase credibility of obtained data. It can be noticed that the most artifacts (but not all) are sources of weak echos. Kuc proposed a method to eliminate them using a standard Polaroid sonar. The 6500 ranging module controlling a Polaroid sonar can detect echoes beyond the initial one by resetting the detection circuit. The device specification suggests inserting a delay before resetting to prevent the current echo

from retriggering the detection circuit. Ignoring this suggestion, Kuc applied another method. He repeatedly reset the module immediately after each detection to generate a dense sequence of detection times Kuc, (2001).
Another approach to artifacts elimination is based on the assumption that multi-reflected echos usually comes from the direction being far from the acoustic axis of the sender. This assumption is based on the observation that that the emitted signal in such a direction is weaker comparing with the signal propagated in the direction of the acoustic axis. In consequence it cannot be expected that a strong echo will come from these directions. To determine the direction of echo arrival a binaural sonar system is needed which contains a receiver and a transducer working as a sender and a receiver. Kreczmer, (1998). However more efficient

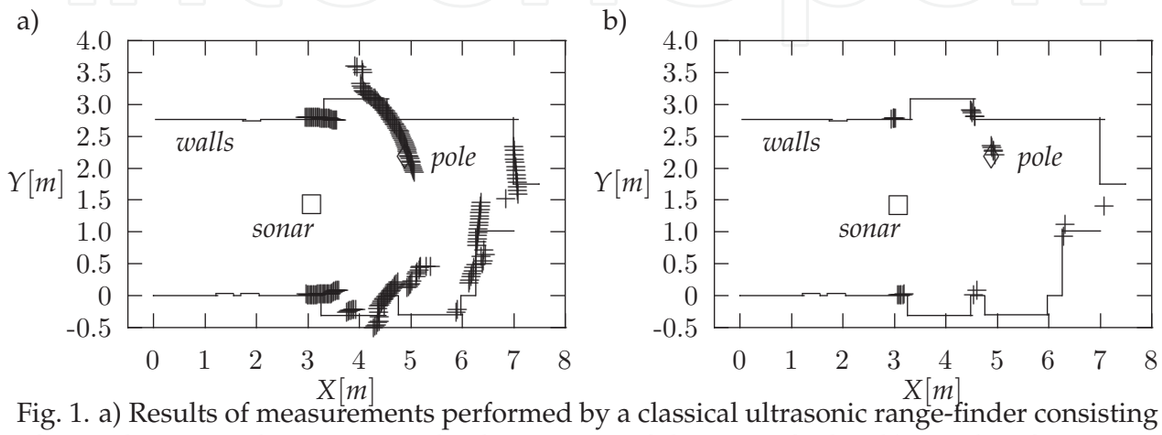

Fig. 1. a) Results of measurements performed by a classical ultrasonic range-finder consisting of a single sonar. The square marks the position of the range-finder. b) Results of measurements performed by a tri-aular sonar system

solution is a tri-aular sonar system which works as a double binaural system (two receivers and a single transducer working as a sender and receiver) The result obtained from the second pair of sonars can be used as a confirmation result obtained from the first one. It allows to reject some week echos. This solution combining with restriction to echos coming from direction being close to the acoustic axis of the system creates an efficient filter. It makes possible significantly to increase credibility of obtained data. The example of a such case is presented in fig. 1. The data obtained from an ultrasonic range-finder consisting of a single sonar are shown in fig. 1a. The range-finder scanned the surrounding at every 0.9°. It has

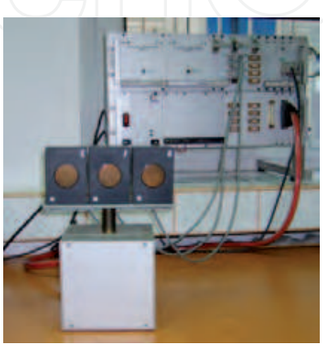

Fig. 2. The tri-aular sonar system

been built using a standard Polaroid transducer 600–series model and a ranging module series 6500. Measurements for the same scene have been performed using a tri-aural system (see fig. 2). The obtained results are presented in fig. 1b. The area around the acoustic axis of the system has been restricted up to $\pm 4^{\circ}$. It allowed successfully to reject most of false reading. Unfortunately some correct echos have been also rejected due to error measurements. The construction of the tri-aular sonar system has been also based on Polaroid transducers 600–series model and the 6500 ranging modules. These modules stimulate the transducer by series of 16 pulses in order to force it to emit ultrasonic signal. Then after $440\mu s$ it can be switched into a receiver mode. The module doesn't allow to start receiving without sending a signal. It is done due to necessary polarization (about $200V$) which has to be set to the electro static transducer. It is needed when the transducers works as an receiver also as a sender. To obtain such a polarization, initial pulses generated during sending mode are used for pumping electric charge. Because in the tri-aular sonar system two side sonars must work only as receivers therefore these modules were modified.

Using multi-sonar system not only some artifacts can be rejected but first of all objects can be much more precisely localized. Moreover some objects can be distinguished. There are three the most elementary reflectors: a wall, a 90° concave corner and a convex edge. In Peremans et al., (1993) it was presented a method which makes possible to localize and classify an edge and a wall. A corner and a wall are indistinguishable in this approach. The method is based on measurements of TOF. In the aforementioned paper a tri-aular sonar system was proposed to solve the problem of the object localization and classification.

An other approach was proposed in Kleeman & Kuc, (1995). In this approach a sonar system which consists of three ultrasonic transducers is also used and TOF is measured. But they are in different way arrange. Additionally two of them are used as transmitters and all of them are used as receivers. Kleeman and Kuc showed that to distinguish wall, edge and corner, measurements performed by using at least two transmitters located in different places are needed. Therefore in their system two measurements are performed. The cases discussed so far can regarded as 2D cases. In Akbarally & Kleeman, (1995) the described method was extended to 3D case. The constructed sonar system consisted of five ultrasonic transducers. A binaural sonar system for object differentiation was presented in Ayrulu et al., (1997). It consisted of two receivers and two transmitters. The sonar system was able to measure TOF and an echo amplitude. Objects features were generated as being evidentially tied to degrees of belief which were subsequently fused by employing multiple logical sonars at different geographical sites. Feature data from multiple logical sensors were fused with Dempster-Shafer rule of combination to improve the performance of classification by reducing perception uncertainty. Dempster-Shafer fusion results were contrasted with the results of combination of sensor beliefs through simple majority vote. A different approach is presented in Heale & Kleeman, (2001). It is based on the Maximum Likelihood Estimation technique. To perform the localization and classification task a real time DSP-based sensing module was constructed. It made possible to apply a double pulse coding method. This approach was extended in order to take into account robot movement Kleeman, (2004).

The object position determination in 3D coordinate system is a bit more complicated. It can be shown that to distinguish edge, corner, wall and point-like object, measurements performed by using at least three transmitters and receivers are needed Kreczmer, (2006). If they can also work as receivers then the system can be restricted up to three ultrasonic transducers. It seems to be the minimal configuration. This kind of system was also applied by Li & Kleeman, (1995) to differentiate walls and corners. In Jimenez et al., (2005) a classification method based on

the principal component-analysis technique was proposed. A sonar system which was used in implementation of the method consisted of eight ultrasonic transducers. In Ochoa et al., (2009) approach was improved and the sonar system reduced two four transducers.
Another crucial point in the problem of object localization and differentiation is the accuracy of echo detection. The currently reported precision is about $1mm$ e.g. Egaa et al., (2008) Angrisani & Moriello, (2006) which is satisfying for many applications.

3. Object localization by binaural sonar system

The basic technique for object localization using TOF is the well known triangulation method. The system applying this method has to consist of at least two receivers and a single emitter. It can be also used a single receiver and a transducer which can work as an emitter and a receiver. To reduce the error of object position determination both receivers have to be placed as far as possible from each other. But there are additional conditions which limit the distance between them. If the distance is too big, it can happen that the echo will be received mostly by only a single receiver. Another case arises when there are a lot of objects in the robot environment. To large baseline of the sonar system can cause that receivers register an echo which hasn't been produced by the same object. This is the reason while the distance between sonars cannot be uniquely determined. It must be adjusted to an environment in which the robot operates, and to the expected maximal range of distance to an object which should be localized. The length of the baseline must be also adjusted to measurement errors.
The simples case of object position determination is an edge or a narrow pole (see fig. 3). The

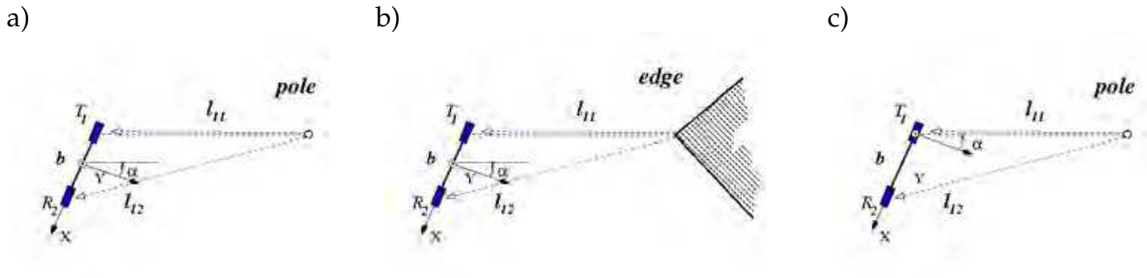

Fig. 3. The bird's-eye view of the signal paths for a) a pole, b) an edge, c) a pole and the coordinate system placed at T_1

distance of a path flown by an ultrasonic wave from the emitter T_1 and back to T_1 switched to the receiver mode, is l_{11}. The length of the signal path from T_1 to the receiver R_2 is l_{12}. Applying a triangulation method the Cartesian coordinates of the object can be determined using simple formulae

$$x = \frac{1}{2b} l_{12}(l_{11} - l_{12}), \qquad y = \frac{1}{2}\sqrt{l_{11}^2 - \frac{1}{b^2}(l_{12}(l_{11} - l_{12}) + b^2)^2}. \tag{1}$$

They are derived for the local coordinate system placed in the middle of the sonar system (see fig. 3a,b). The polar coordinates of the object are determined by formulae

$$r = \frac{1}{2}\sqrt{(l_{11} - l_{12})^2 + l_{12}^2 - b^2}, \qquad \alpha = \arcsin \frac{l_{12}(l_{11} - l_{12})}{b\sqrt{(l_{11} - l_{12})^2 + l_{12}^2 - b^2}}. \tag{2}$$

It is assumed that the angle α is measured from the axis OY in the anticlockwise direction. In the coordinate system of the transmitter (see fig. 3c) the formula for r becomes extremely simple. All formulae in this coordinate system are as follows

$$x = \frac{1}{2b}(l_{12}(l_{11} - l_{12}) + b^2), \qquad y = \frac{1}{2}\sqrt{l_{11}^2 - \frac{1}{b^2}(l_{12}(l_{11} - l_{12}) + b^2)^2}.$$

$$r = \frac{l_{11}}{2}, \qquad \alpha = \arcsin\frac{1}{bl_{11}}(l_{12}(l_{11} - l_{12}) + b^2). \tag{3}$$

For a wall the paths of an received echos are a bit more complicated (see fig. 4a). The inclination angle of the signal coming back to T_1 is always equal to 90°. For the signal received by R_2 the inclination and reflection angle are the same. This is due to the assumption that irregularities of an object surface are much smaller than the wave length of the emitted signal. The analyze is much more easier if the approach of the virtual image of the sonar system is

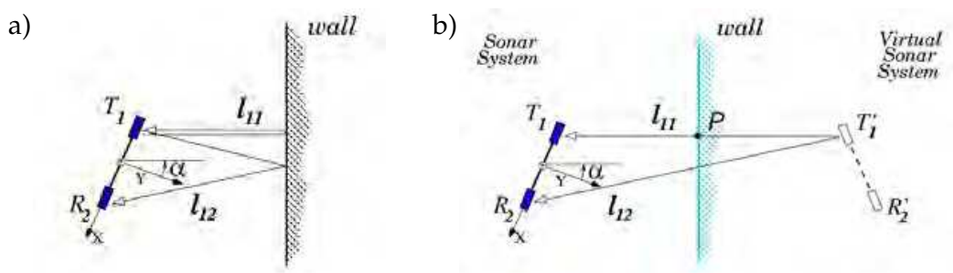

Fig. 4. a) The bird's-eye view of the signal paths for a wall. b) The symmetrical image of the sonar system allows to simplify the signal paths analysis

applied. The construct of virtual images is borrowed from an optical context and is used by many researches Peremans et al., (1993)Kleeman & Kuc, (1995)Heale & Kleeman, (2001). The virtual image of a transducer in a plane is obtained by reflecting the true position of the transducer about the plane. In this way the wall introduce a plane symmetry (see fig. 4b). The location of the point P can be easily determined. Its Cartesian coordinates in the local coordinate system of the binaural sonars range-finder are

$$x = \frac{1}{4b}(l_{11}^2 - l_{12}^2 - b^2), \qquad y = \frac{1}{2}\sqrt{l_{11}^2 - \frac{1}{4b^2}(l_{11}^2 - l_{12}^2 + b^2)^2}. \tag{4}$$

In the polar coordinate system the components of coordinates can be expressed as follows

$$r = \frac{l_{12}}{2}, \qquad \alpha = \arcsin\frac{1}{2bl_{12}}(l_{12}^2 - l_{11}^2 + b^2). \tag{5}$$

This time the formula for r is simple in the both coordinate systems i.e. the coordinate system placed in the middle of the baseline (see above) and the coordinate system combined with the sonar T_1. The formulae expressed in the last mentioned coordinate system are presented below

$$x = \frac{1}{4b}(l_{11}^2 - l_{12}^2 + b^2), \qquad y = \frac{1}{2}\sqrt{l_{11}^2 - \frac{1}{4b^2}(l_{11}^2 - l_{12}^2 + b^2)^2},$$

$$r = \frac{l_{11}}{2}, \qquad \alpha = \arcsin\frac{1}{2bl_{11}}(l_{12}^2 - l_{11}^2 - b^2).$$

Because l_{11} is perpendicular to a surface of a wall the straight line equation of a vertical cast of a wall can be determined.
The next very characteristic reflector is a corner. It is an example of surfaces arrangement which is the source of double reflections (see fig. 5a). The virtual image of a transducer in a

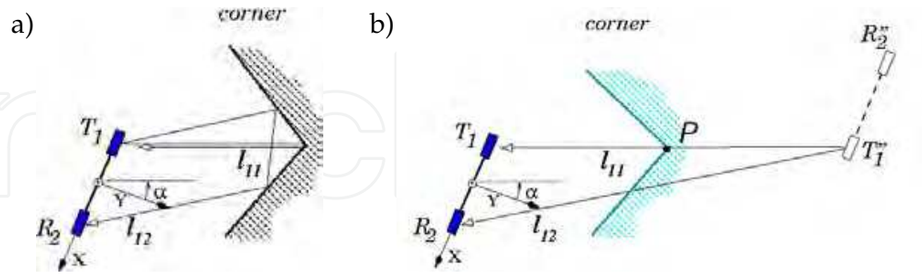

Fig. 5. a) The bird's-eye view of the signal paths for a corner. b) Signal path after creating a virtual sonar system being an image of the real system using axial symmetry

corner is obtained by reflecting about one plane and then the other which results in a reflection about the line of intersection of the planes. Thus finally the axial symmetry is obtained. This kind of symmetry is also obtained for the edge case. The only difference is that drawing signal path from a virtual sonar to a real one the path must always cross the edge (see fig. 7a). In this sens it isn't the same technique which is used for a wall or a corner. Considering 2D case the coordination of the point P can be determined (see fig. 5b). The obtained measurements results don't allow to determine the location of both walls. It doesn't depend on the number of senders and receivers. It is clear when two different corner orientations are considered (see fig. 6). For both orientations the same virtual image of sonar system is obtained. The position

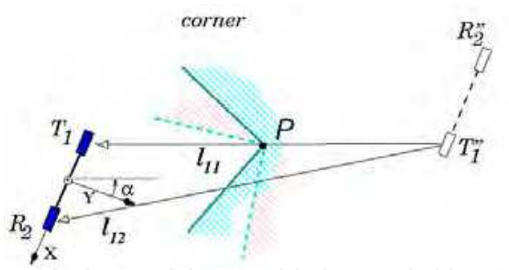

Fig. 6. The same virtual image of the sonar system is created for two different orientation of the corner

of the point P can be computed using (4) and (5). It means that the formulae can be applied which are used for a wall.

4. Object classification

Because the formulae allowing to determine object location are different for edges, walls and corners, to determine correctly the object position first it should be recognize and properly classified. Data obtained from a single measurement aren't enough to distinguish objects discussed in this section. It was shown that at least two measurements are necessary by using emitters located at different places Kleeman & Kuc, (1995). It can be done using the binaural sonar system. To do so it is necessary to replace the receiver R_2 with a transducer T_2 working

as an emitter and a receiver. In this form the sonar system makes possible to perform two measurements. The first is done by using T_1 as a transmitter and the second is executed by using T_2. During both measurements the transducers are switched into receiving mode after the signal emissions. Signal paths for all cases are shown in fig. 7. In all sketches of signal

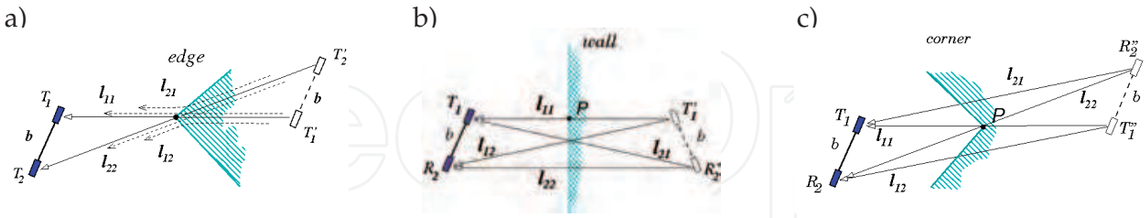

Fig. 7. The virtual images of the sonar system and signal paths for all cases. The edge case differs form the cases of a wall and a corner because signal path from a virtual sonar must cross the point marked the edge

paths the technique of virtual images is exploited. The edge case doesn't follow exactly this technique. But this drawing makes easier to notice some relations.
Considering geometrical figures created by signal paths and sonar systems and their virtual images for each case a single condition can be found. Their are as follows

$$\begin{array}{lcrcl} \textit{edge} & \rightarrow & l_{12}+l_{21}-l_{11}-l_{22} & = & 0, \\ \textit{wall} & \rightarrow & (l_{12}+l_{21})^2-4b^2-4l_{11}l_{22} & = & 0, \\ \textit{corner} & \rightarrow & (l_{12}+l_{21})^2+4b^2-2l_{11}^2-2l_{22}^2 & = & 0. \end{array} \tag{6}$$

It can be added another condition $l_{12}-l_{21}=0$. But it isn't combined directly with arrangement of signal paths. It is rather a general feature. The presented condition can be used for object distinguishing. In Heale & Kleeman, (2001) the Maximum Likelihood Estimation classification approach has been applied which was based on the conditions presented above. But if an measurement error can be limited to a certain range a simpler method can be proposed. At the beginning let us consider a possibility of using of the edge condition as a criterion of reflector classification, i.e.

$$C_e(O_i,b)=l_{11}+l_{22}-l_{12}-l_{21}.$$

where O_i is an object being source of echos, b is the distance between sonars. l_{11},l_{22}, l_{12}, l_{21} are measured distances which are the functions of object type, its location and the length of the baseline b.
Analyzing fig. 7a and fig. 7c it can be easily noticed that for a corner it must be $C_e(O_c,b)\geq 0$. But the condition $C_e(O_c,b)=0$ is met only for the orientation of the sonar system: $\alpha=-90^\circ$ or $\alpha=90^\circ$. These configurations aren't needed to be taken into account. It is caused by the fact that if a direction to an object is far from the direction of the transmitter acoustic axis then an amplitude of an emitted signal is equal to 0 or almost 0. Thus for all reasonable configurations the condition $C_e(O_c,b)>0$ must be held.
For the wall case fig. 7a and fig. 7b should be considered. It can be found out that $C_e(O_w,b)\leq 0$. But $C_e(O_w,b)=0$ is in the same situations like for a corner. For the same reasons it can be assumed that for all possible configurations it should be $C_e(O_w,b)<0$. The deduced features of $C_e(O_i,b)$ allows it to be a good candidate for the criterion distinguishing edges, walls and corner.

To prove the discussed feature the function $C_e(O_w, b)$ can be derived using the parameterization by d and α where d is the distance to a wall from the sonar system and α is its orientation in relation to the wall (see fig. 3)

$$C_e(O_W, b) = C_{e,W}(d, \alpha, b) = 2\sqrt{4d^2 + b^2\cos^2\alpha} - 4d. \tag{7}$$

The same type of parameterization can be used for a corner. It gives

$$C_e(O_C, b) = C_{e,C}(d, \alpha, b) = 4d - \sqrt{(2d - b\sin\alpha)^2 + b^2\cos^2\alpha} - \sqrt{(2d + b\sin\alpha)^2 + b^2\cos^2\alpha}. \tag{8}$$

The example of the function plots for $C_e(O_{C_k}, b)$ and $C_e(O_{W_k}, b)$ is presented in fig. 8. These

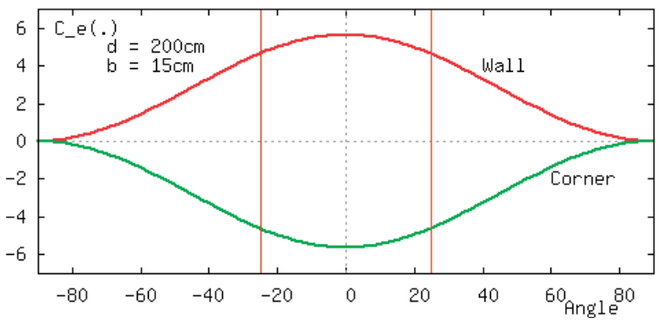

Fig. 8. The values of the criterion C_e for a wall and a corner. The charts are drawn for a system placed $2m$ from an object and sonars placed in the distance $15cm$ to each other

plots confirm the previous deduction based on geometric shapes of the paths. The chart shows that for $|\ \alpha\ | > 60^\circ$ the values of $C_e(O_{C_k}, b)$ and $C_e(O_{W_k}, b)$ are very close to 0. But the full range of orientation isn't necessary to take into account. Because the width of the emitted beam is restricted to about $40^\circ \sim 50^\circ$, the range of considered orientations can be confined to $[-25^\circ, 25^\circ]$. It gives an additional advantage because in this range the functions reach values which are very close to the extrema ones. That makes possible to distinguish all considered objects.

It can be expected that it is easier to distinguish the object when it is close than it is far. In other words it means that the values of $C_e(O_E, b)$, $C_e(O_W, b)$ and $C_e(O_W, b)$ should be close to each other when the distance to objects is small. The difference should be increased when the distance is large. Because $C_e(O_E, b)$ for all distance equals to 0, the presented feature means that for large distances, values of $C_e(O_W, b)$ and $C_e(O_C, b)$ are more apart from 0. This feature can be observed on charts presented in fig. 9. The analogous feature can be noticed while the distance b between sonars is considered. The larger baseline b the more extreme values by $C_e(O_W, b)$ and $C_e(O_C, b)$ are reached (see fig. 10).

In the following part the stable conditions in the environment are assumed. It means that in the surrounding where the sonar system operates there are no wind, no very hot spots etc. It allows us to assume that the maximal measurement error Δl can be estimated and is the same for all l_{ij}. Thus the error of $C_e(O_i, b)$ is

$$\Delta C_e(O_i, b) = \left(\left|\frac{\partial C_e}{\partial l_{11}}\right| + \left|\frac{\partial C_e}{\partial l_{12}}\right| + \left|\frac{\partial C_e}{\partial l_{21}}\right| + \left|\frac{\partial C_e}{\partial l_{22}}\right|\right)\Delta l + \left|\frac{\partial C_e}{\partial b}\right|\Delta b = 4\Delta l.$$

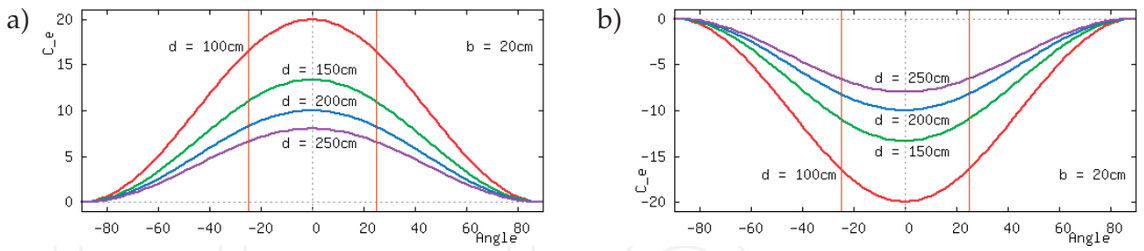

Fig. 9. The values of the criterion C_e for a wall and a corner. The charts are drawn for a system placed at different distances from an object and sonars separation distance $b = 20cm$

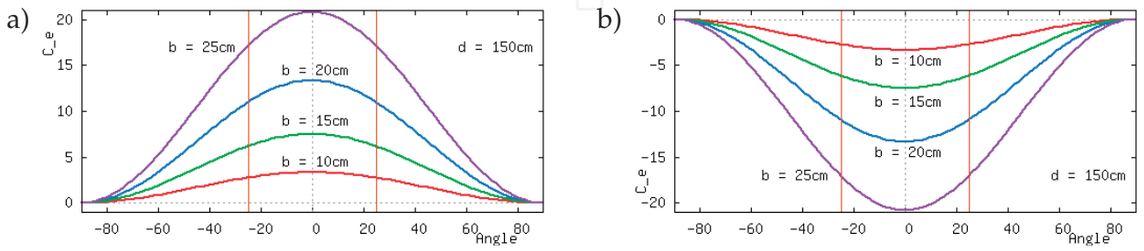

Fig. 10. The values of the criterion C_e for a wall and a corner. The charts are drawn for a system placed at $1.5m$ from and object and different distances between sonars

It means that if an object must be properly distinguished at the distance d_{max}, the value b must be enough big in order to obtain

$$C_{e,W}(d_{max}, \alpha_{max}, b) > 8\Delta l \quad \wedge \quad C_{e,C}(d_{max}, \alpha_{max}, b) < 8\Delta l.$$

where α_{max} is the biggest value of the assumed orientation range. In the considered example it has been assumed $\alpha_{max} = 25^{\circ}$. The equations presented above is the necessary condition but not sufficient one. The example of proper choice of b for $d_{max} = 1.5m$ is presented in fig. 11. It shows the drawing of $C_{e,W}$ and $C_{e,C}$ with *tunnels* of acceptable values. The classification

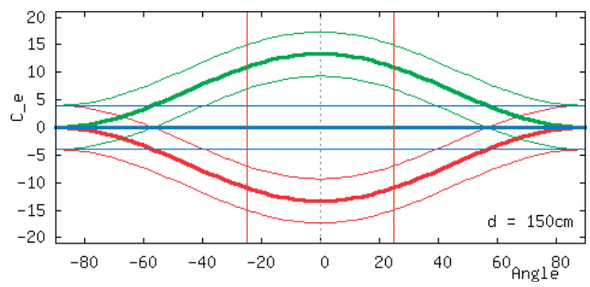

Fig. 11. The values of the criterion C_e for a corner, an edge and a corner. In the chart, ranges of acceptable values in the sens of error measurement are marked

procedure which includes sufficient conditions can be described by the rules:

$$\begin{array}{llll} if & C_e(O_i,b) \in (-4\Delta l,\ 4\Delta l) & \Rightarrow & \text{edge}, \\ if & C_e(O_i,b) \in (C_{e,W}(d,\alpha,b) - 4\Delta l,\ C_{e,W}(d,\alpha,b) + 4\Delta l) & \Rightarrow & \text{wall}, \\ if & C_e(O_i,b) \in (C_{e,C}(d,\alpha,b) - 4\Delta l,\ C_{e,C}(d,\alpha,b) + 4\Delta l) & \Rightarrow & \text{corner}, \\ & otherwise & \Rightarrow & \text{unknown}. \end{array} \tag{9}$$

This set of rules seems to contain a dead loop. To classify an object properly its position must be known. But to determine properly the position of the object it must be first classified. Fortunately the difference of paths length between the edge and wall case is small. Therefore the procedure applied for an edge can be also used for a wall and a corner. The error of the angle α for wall localization is about 0.5° while the distance between sonars is $8cm$ and the wall is at the distance $2m$. The error is increased to about 1° when the distance between sonars is increased up to $16cm$. The error of distance computing is negligible. In this way the very good approximation of the real position can be obtained. But it is still possible to improve it. It can be noticed that for a wall when T_1 is used as an emitter, the hypothetical reflecting edge is a bit on the left in relation to the correct direction to the wall (see E_1 in fig. 12a). When T_2 is used as an emitter, the the hypothetical reflecting edge is on the opposite site almost with the same angle (see E_2 in fig. 12a). For a corner the final result is similar. The only difference is that

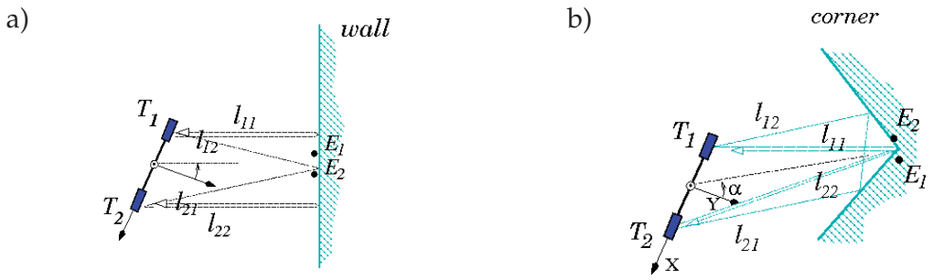

Fig. 12. The determined positions of hypothetical objects when the triangulation procedure is applied for measurements obtained for the wall case

the positions of hypothetical edges are reversed comparing with the wall case. This feature is exploited in Heale & Kleeman, (2001) for object distinguishing. The important disadvantage of the method is that it doesn't allow easily to take into account errors of measurements and set a proper margin of acceptable values.

The computed locations of hypothetical edges make possible quite precisely to determine the position of the object. Because the previously discussed errors of the hypothetical edges have opposite value, it is enough to compute the mean of these locations to obtain the position of the object. It reduces the error of the angle α to about 0.1°. This is for the worst case when object is located at the distance $2m$ with the bearing angle 25°. The best case is for bearing 0°. It gives exactly symmetrical configuration which cancels the error. Because even for the worst case the bearing error is very small, it can be neglected.

This procedure also reduces the error of bearing determination caused by measurements error of l_{ij}. If the interval between the successive sonars firing T_1 and T_2 is short, then distance measurement is highly correlated Heale & Kleeman, (2001). Therefore the measurement error is usually much lower than the assumed error of a single separate measurement. Nevertheless this kind of the bearing error must be taken into account for a wall and a corner classification because $C_{e,W}$ and $C_{e,C}$ depend on α. In this sense it isn't needed to be considered for $C_e(O_E, b)$. The criterion value for an edge is constant for each orientation of the sonar system. Thus it doesn't depend on the bearing angle.

The error of the α determination can cause that some acceptable values can be shifted outside the *tunnel* of the expected values. Moreover, some unacceptable values can be moved into the tolerance *tunnel* of measured values. Thus if we want to be sure that the classification is proper in the sens of assumed measurements error, the *tunnels* of acceptable values must

be narrowed. Considering this part of acceptable range which is shifted outside the tunnel, it is also necessary to widen the tunnel. The area between the border of the narrowed and widened tunnel contains values for which an object can be a wall but not for sure (in the sens of the assumed measurement error). To clinch it a next measurement has to be perform. The area outside the tunnel contains values which indicate that an object isn't a wall for sure.
Taking into account the aforementioned arguments it allows us to create the border of the narrowed tunnel. The top and bottom border of this area can be defined as follows

$$\overline{C}_{W,nar}(d,\alpha,b) = \begin{cases} C_{e,W}(d,\alpha-\Delta\alpha,b)+4\Delta l & \alpha < \Delta\alpha \\ C_{e,W}(d,0,b)+4\Delta l & \alpha \in [-\Delta\alpha,\Delta\alpha] \\ C_{e,W}(d,\alpha+\Delta\alpha,b)+4\Delta l & \alpha > \Delta\alpha \end{cases}$$

$$\underline{C}_{W,nar}(d,\alpha,b) = \begin{cases} C_{e,W}(d,\alpha+\Delta\alpha,b)-4\Delta l & \alpha < \Delta\alpha \\ C_{e,W}(d,0,b)-4\Delta l & \alpha \in [-\Delta\alpha,\Delta\alpha] \\ C_{e,W}(d,\alpha-\Delta\alpha,b)-4\Delta l & \alpha > \Delta\alpha \end{cases}$$

In similar way the border of the widened tunnel can constructed. The same procedure and analogically definitions can be used to construct the tunnels of acceptable values for a corner. This approach suffers the main important disadvantage. The value of $\Delta\alpha$ also depends on the measured distances l_{ij}. Furthermore the formula of $\Delta\alpha$ is very complicated. Thus such an approach cannot be easily implemented.
The advantage of using C_e is that for an edge it doesn't depend on α. Therefore their values doesn't depend on $\Delta\alpha$. Unfortunately, as it has been shown, the same arguments cannot be used for corner and wall cases.
In the same way as the edge criterion has been defined, the criterion for a wall can be constructed. Using the second equation from (6) the criterion can be defined as follows

$$C_w(O_i,b) = (l_{12}+l_{21})^2 - 4b^2 - 4l_{11}l_{22}.$$

The analogical criterion can be defined for a corner using the third equation from (6)

$$C_c(O_i,b) = (l_{12}+l_{21})^2 + 4b^2 - 2l_{11}^2 - 2l_{22}^2.$$

The error of C_w can be approximated by the formula

$$\Delta C_w = \Big(\Big|\frac{\partial C_w}{\partial l_{11}}\Big| + \Big|\frac{\partial C_w}{\partial l_{12}}\Big| + \Big|\frac{\partial C_w}{\partial l_{21}}\Big| + \Big|\frac{\partial C_w}{\partial l_{22}}\Big|\Big)\Delta l + \Big|\frac{\partial C_w}{\partial b}\Big|\Delta b = 4(l_{11}+l_{12}+l_{21}+l_{22})\Delta l + 8b\Delta b. \tag{10}$$

Expressing the measured lengths of signal paths l_{ij} as functions of d and α for the wall case, the following formulae are obtained

$$\begin{aligned} l_{11} &= 2d + 2b\sin\alpha, \\ l_{22} &= 2d - 2b\sin\alpha, \\ l_{12} = l_{21} &= \sqrt{4d^2 + b^2\cos^2\alpha}. \end{aligned}$$

Applying these expressions to the formula (10) it gives

$$\Delta C_w = (16d + 8\sqrt{4d^2 + b^2\cos^2\alpha})\Delta d + 8b\Delta b.$$

Because $d \gg b$ and $\Delta d \geq \Delta b$ then

$$\Delta C_w \simeq 32d\Delta l.$$

Thus ΔC_w can be considered as independent on α. It can be noticed that C_w has the similar feature for a wall as C_e for an edge (see fig. 13a). Considering C_c the same formula is obtained

$$\Delta C_c = \Big(\Big|\frac{\partial C_c}{\partial l_{11}}\Big| + \Big|\frac{\partial C_c}{\partial l_{12}}\Big| + \Big|\frac{\partial C_c}{\partial l_{21}}\Big| + \Big|\frac{\partial C_c}{\partial l_{22}}\Big|\Big)\Delta l + \Big|\frac{\partial C_c}{\partial b}\Big|\Delta b = 4(l_{11} + l_{12} + l_{21} + l_{22})\Delta l + 8b\Delta b.$$

This time the measured lengths of signal paths l_{ij} have to be expressed for the corner case as functions of d and α. It gives formulae

$$\begin{aligned} l_{11} &= \sqrt{4d^2 + b^2 \sin\alpha}, \\ l_{22} &= \sqrt{4d^2 - b^2 \sin\alpha}, \\ l_{12} = l_{21} &= 2d. \end{aligned} \tag{11}$$

Direct substitution to (11) and computing derivations yields

$$\Delta C_c = (16d + 4\sqrt{4d^2 + b^2 \sin\alpha} + 4\sqrt{4d^2 - b^2 \sin\alpha})\Delta l + 8b\Delta b.$$

Using the same arguments as before i.e. $d \gg b$ and $\Delta d \geq \Delta b$, the final approximation is obtained

$$\Delta C_c \simeq 32d\Delta l.$$

It allows us to draw charts of C_w and C_c and mark *tunnels* of acceptable values. It is done in the same way as it has been done for C_e. Fig. 13 presents these charts. It can be noticed

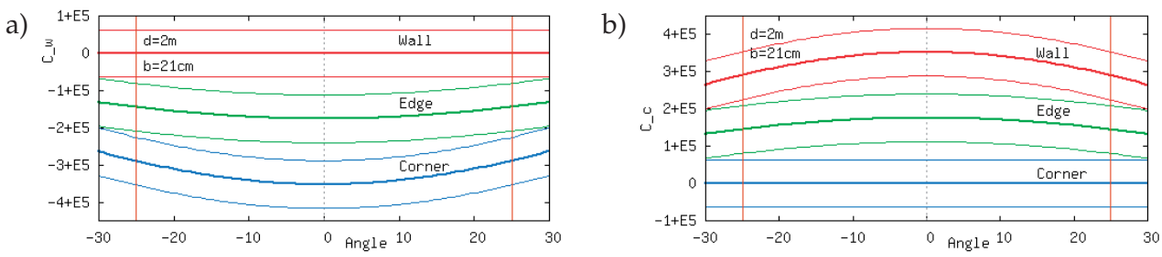

Fig. 13. Charts of C_w and C_c being drawn for a wall, an edge and a corner. Around them ranges of acceptable values for proper classification are marked

that the range of the proper separation of all cases is preserved (compare fig. 13 and fig. 14). Therefore it is enough to analyze only a single criterion in order to determine the initial length of the baseline b which guarantees the correct classification of the considered objects at a given

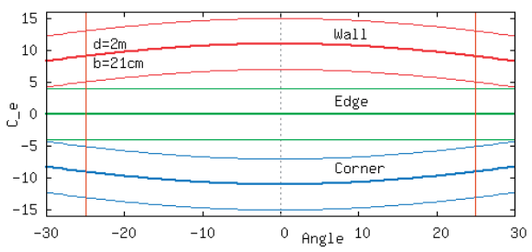

Fig. 14. Charts of C_e being drawn for a wall, an edge and a corner. Around them ranges of acceptable values for proper classification are marked

distance. But to classify an object all criterion have to be taken into account in order to avoid any ambiguity. The procedure of classification can be written as a set of rules

$$\begin{array}{lcll} \mid C_e(O_i) \mid \leq 4\Delta l \ \wedge & \mid C_w(O_i) \mid > 32d\Delta l \ \wedge & \mid C_c(O_i) \mid > 32d\Delta l & \Rightarrow \quad edge, \\ \mid C_e(O_i) \mid > 4\Delta l \ \wedge & \mid C_w(O_i) \mid \leq 32d\Delta l \ \wedge & \mid C_c(O_i) \mid > 32d\Delta l & \Rightarrow \quad wall, \\ \mid C_e(O_i) \mid > 4\Delta l \ \wedge & \mid C_w(O_i) \mid > 32d\Delta l \ \wedge & \mid C_c(O_i) \mid \leq 32d\Delta l & \Rightarrow \quad corner, \\ & & \text{otherwise} & \Rightarrow \quad \text{unknown}. \end{array} \tag{12}$$

It is worth to note that the procedure doesn't require to use trigonometric functions or square root operations. Therefore it can be implemented using a low cost controller which doesn't support float point arithmetic.
Another important feature is combined with the set of equations (6). It can be noticed that all of them it is possible to obtain from a single general equation

$$(l_{12}+l_{21})^2-(l_{11}+l_{22})^2+\rho\Big((l_{11}-l_{22})^2-4b^2\Big)=0$$

where $\rho \in [-1,1]$. The equation for a corner is obtained for $\rho=-1$. The values 0 and 1 make possible to obtain the equations for an edge and a wall respectively. Thus instead of using the rules (12) the ρ value can be computed and in this way an object can be classified.

5. Simplified triangulation method for object location

The method of object distinguishing presented in the previous section has very important advantage. It can be implemented without using float point arithmetic. This method doesn't use trigonometric functions or square root operations. In this way low cost processors can be used to create a more intelligent sensor. But this advantage is lost when we want to combine this approach with the location method based on triangulation procedure. The formulae (1) and (2) requires such a function and an operation. In this section a method is presented which makes possible to omit this problem. It allows to reduce the necessary computation power and in this way it makes possible to construct a cheap intelligent sensor which can determine the location of an object and can classify it.
The presented approach is based on the method described in Kuc, . The main idea of the approach consists in determining a pass distance between an obstacle and a mobile robot moving along a straight line. Successive results of measurement are used in order to compute an object position. The pass distance y_p (see fig. 15a) can determined using the equation (13).

$$y_p = \sqrt{r_d^2 - x_p^2} \tag{13}$$

Assuming that the measurements are performed in placed which are regularly spread along the straight line (see fig. 15b) the pass distance can expressed by the formula (14). Building this formula it is also assumed that the object is passed by at the point determined by $k=0$.

$$y_{p,k} = \sqrt{r_k^2 - (kd_s)^2} \tag{14}$$

Considering a sequence of three places the computed values of y_p can be expressed by the set of equations (15).

$$\begin{array}{rcl} y_{p,k} & = & \sqrt{r_k^2 - (kd_s)^2} \\ y_{p,k-1} & = & \sqrt{r_{k-1}^2 - ((k-1)d_s)^2} \\ y_{p,k-2} & = & \sqrt{r_{k-2}^2 - ((k-2)d_s)^2} \end{array} \tag{15}$$

Fig. 15. a) A robot equipped with an ultrasonic sonar moves along a straight line and passes by an object. b) The measurements of the distance to an object are performed at the points regular spread along the robot path

It is more convenient to compute y_p^2 instead of y_p. The differences of y_p^2 for each two following points are presented by formulae (16)

$$\begin{aligned} y_{p,k}^2 - y_{p,k-1}^2 &= r_k^2 - r_{k-1}^2 - 2kd_s^2 + d_s^2 \\ y_{p,k-1}^2 - y_{p,k-2}^2 &= r_{k-1}^2 - r_{k-2}^2 - 2kd_s^2 + 3d_s^2 \end{aligned} \tag{16}$$

The computed values $y_{p,k}, y_{p,k-1}, y_{p,k-2}$ should meet the condition $y_{p,k} = y_{p,k-1} = y_{p,k-2} = y_p$. In this way we obtained.

$$\begin{aligned} 0 &= r_k^2 - r_{k-1}^2 - 2kd_s^2 + d_s^2 \\ 0 &= r_{k-1}^2 - r_{k-2}^2 - 2kd_s^2 + 3d_s^2 \end{aligned} \tag{17}$$

These formulae allow us to determine k parameter.

$$\begin{aligned} k &= \tfrac{1}{2d_s^2}(r_k^2 - r_{k-1}^2) + \tfrac{1}{2} \\ k &= \tfrac{1}{2d_s^2}(r_{k-1}^2 - r_{k-2}^2) + \tfrac{1}{2} + 1 \end{aligned} \tag{18}$$

The general form of a formula exploiting r_{k-l} and r_{k-l-1} is presented below

$$k = \frac{1}{2d_s^2}(r_{k-l}^2 - r_{k-l-1}^2) + \frac{1}{2} + l. \tag{19}$$

This formula can be still simplified while we take into account a method of distance determination. The most popular method is based on time measurement of a signal flight (TOF). Because the time is measured by digital clock, the measured distance can expressed as follows

$$r = \frac{c_s \Delta t}{2} = \frac{c_s(p\Delta\tau)}{2} = p\frac{c_s \Delta\tau}{2}$$

where $\Delta\tau$ is an elementary slice of time measured by clock, m is the number of elementary time slices. We can arbitrary choose the duration of the elementary slice $\Delta\tau$. Thus we can choose the value of the slice in order to meet the equation (20)

$$d_s = \frac{c_s \Delta\tau}{2}. \tag{20}$$

It allows us to simplify the formula (19) as follows

$$k = \frac{1}{2}(p_{k-l}^2 - p_{k-l-1}^2 + 1) + l \tag{21}$$

where m_{k-l} and m_{k-l-1} are the numbers of time slices counted while the distances r_{k-l} and r_{k-l-1} are measured. It is worth to note that all elements of the equation (21) are integer numbers. In this way the software implementation can be simplified and it makes even possible a hardware implementation of the approach.
This kind of discretization introduce an error of distance measurement equal: $\Delta r = d_s$. When d_s is big (e.g. $10cm$ or more) this cannot be accepted. It can be reduced by choosing the smaller time quantum $\Delta\tau$ as follows

$$d_s = n\frac{c_s\Delta\tau}{2}.$$

Applying it to (19) it gives

$$k = \frac{1}{2n^2}(q_{k-l}^2 - q_{k-l-1}^2 + 1) + l.$$

The advantage of this formula is obtained when n is a power of 2. It allows to reduce the division arithmetic operation to register shifting.

5.1 Multi-sonar system

The important advantage of the method presented in the previous section is the elimination of artifacts which are sensible to a change of a sender and detector position. Using the method a sonar must be moved within the same distance step by step. When a sonar is mounted on a mobile robot it can be obtained during robot motion. But this solution introduce additional source of errors i.e. the distance measurement of a robot movement. It can be avoid when a set of sonars is used, instead a single moving sonar (see fig. 16). The sonars can be mounted within a regular shift and the error can be drastically reduced. The sonars arrangement cre-

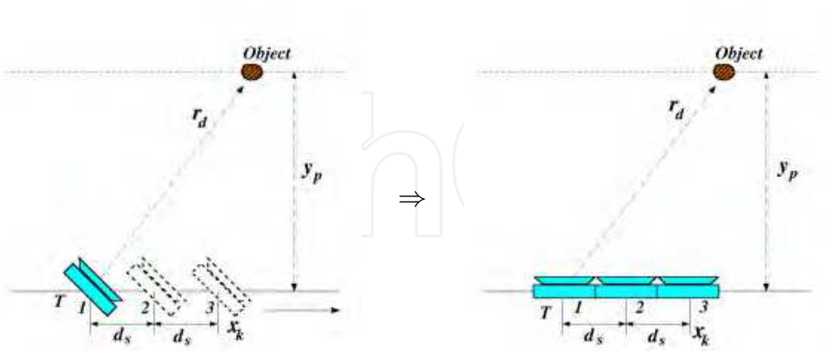

Fig. 16. Instead of regular sonar displacement a sonar array can be used

ates a sonar array. In the simples form it is possible to reduce it to a tri-aular sonar system. Considering the presented method the system can be treated as a double binaural system. The second pair of sonars is used in order to verify the results obtain by the first pair. It shows that the method presented in Kuc, (2007) can be transformed to the known approach which was applied to reduce false sonars reading Kreczmer, (1998). However, the method described

in Kuc, (2007) offers new important benefits in the sense of discretization presented in the previous section. It allows to speed up calculations and makes results more robust.
The method proposed in the previous section introduces an additional error to calculations of the distance y_p. It is caused by discretization. It should be noticed that the step of discretization d_s is quit big. Comparing the approach based on moving a single sonar and tri-aular system it can be shown that the last one has an important advantage. It is due to the orientation of discretized coordinate axis to an object and a sonar acoustic axis. The fig. 16 shows the case when the situation for both systems are exactly equivalent. Because the width of a sonar beam isn't very wide (30° for Polaroid transducers) in order to be noticed an object cannot be far from the acoustic axis of a sonar. When a sonar is pointed towards the movement direction (see fig. 17a), an object cannot be very far from this direction. Considering a tri-aural sonar system or in general a linear array system an object cannot be far from the acoustic axis of the system (see fig. 17b).

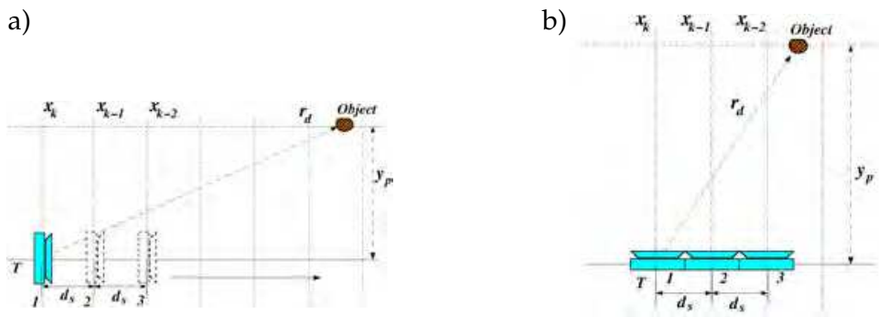

Fig. 17. a) When a sonar is pointed into direction of its movement, an object cannot be far from this direction. Discretization of the distance x_p is applied along the movement direction. b) The object cannot be far from the acoustic axis of the sonar linear array. Discretization of the distance x_p is along the sonar array

The main difference of these two cases is that for a moving sonar $y_p < x_p$ or even $y_p \ll x_p$. The opposite relation is for a multi-sonar system i.e. $y_p \gg x_p$. This feature has very strong impact on an error value of y_p.
Considering the case of moving sonar pointed into the direction of the movement it can be noticed that an error of k being equal to 1 can cause a very big change of the value y_p (see fig. 18a). The same situation considered for a multi-sonar system causes much smaller change of y_p (see fig. 18b) and in consequence much lower error value.
The type of discretization presented in fig. 18b gives an additional advantage. When a value of y_p is needed to be established in order to locate an object in a robot surrounding, the formula (14) should be used. But the value of r_k can be also digitalized and in this way the formula (14) isn't needed any longer to show where the object is. Digitizing x_p and r_k a kind of grid is created (see fig. 19b) which is a mix of Cartesian and polar coordinates discretization. Creating the same type of grid for a sonar pointed towards its movement direction, much bigger cells are obtained. Moreover the angle coordinate is much more fuzzy (see fig. 19a) than for the case of discretization applied to a multi-sonar system. The presented approach to processing of measurement data obtained from a multi-sonar system makes possible to reduce necessary resources of the system controller. Using the final discretized representation of data and a local environment the controller can perform all calculations using only integer data. Which is the very important benefit of the described method.

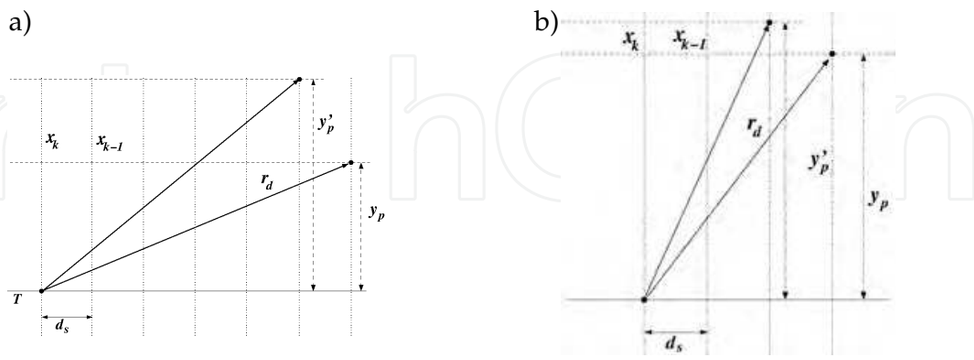

Fig. 18. a) While $y_p \ll x_p$, a small change of k can cause a very big change of value y_p. b) While $y_p \gg x_p$, the same change of k can cause a very little change of value y_p

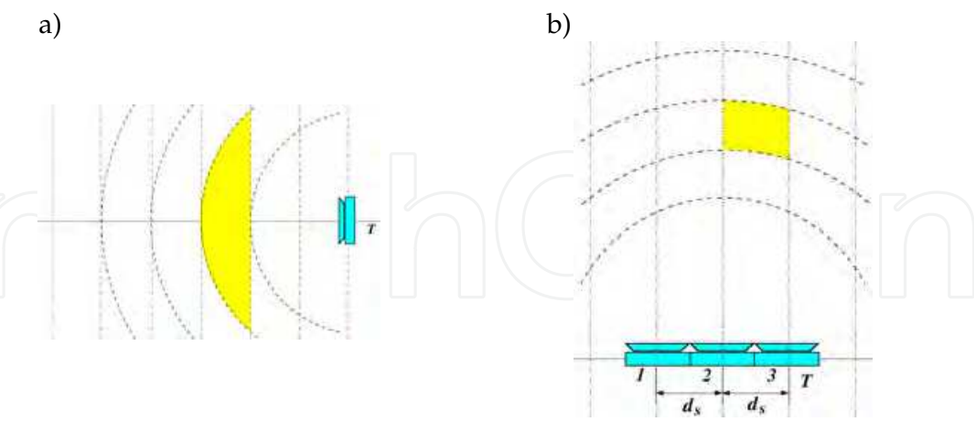

Fig. 19. The mixed Cartesian and polar coordinates discretization for a) a sonar pointed towards its movement direction, b) a multi sonar system

Considering the binaural system it should be assumed that $b = d_s$. But it creates very wide grid cells which is unacceptable (see fig. 20). Fortunately it can be easily solved. Because

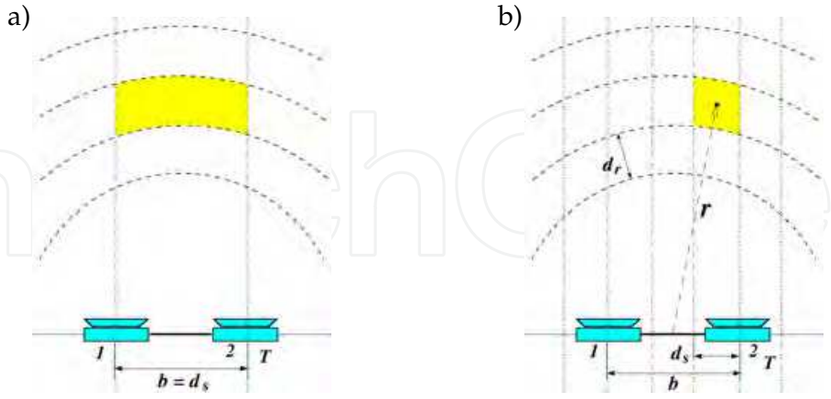

Fig. 20. a) The grid with the big discretization step being equaled to the length b of the baseline of the binaural sonar system. b) More fine discretization where b is a multiplication of d_s.

creating more fine discretization it is obtained

$$b = md_s \quad \Rightarrow \quad \tilde{k}_s = \frac{k}{m}.$$

where m is an positive integer number. It determines the precision of discretization (see fig. 20). Finally it gives

$$\tilde{k}_s = \frac{1}{2n^2m}(q_{k-l}^2 - q_{k-l-1}^2 + m). \tag{22}$$

In this formula comparing it with the formula (19) the parameter l is set to 0 because $\tilde{k}$ is assumed to 0 at the position of the left sonar. Using the binaural sonar system it isn't convenient to apply the discretization in the coordinate system placed in the middle point of the sonars arrangement (see fig. 20a). This approach causes that to compute r value the square root operation is needed. Much efficient approach consist in applying two discretization maps (see fig. 21) representing two look-up tables. They contain coordinates of the cell center expressed

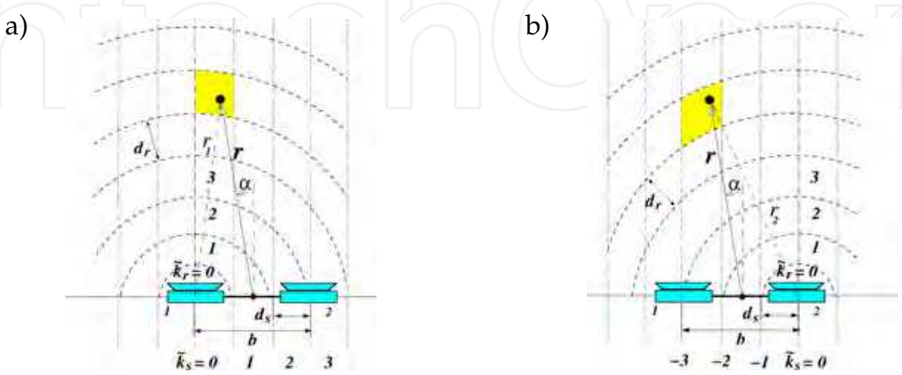

Fig. 21. Interpretation of parameters.

in the coordinates system of the middle of the sonars baseline. Executing two measurements

the final result is the mean of values obtained from these two tables. The values r_1 and r_2 are directly obtained form measurements.

5.2 Basic error analysis

To estimate an computation error of the parameter k the formula (21) has to be considered. This formula shows that the parameter k is a function of r_{k-l}, r_{k-l-1} and d_s. Thus the error can be estimated as follows

$$\Delta k = \frac{1}{d_s^2}(r_{k-l}\Delta r_{k-l} + r_{k-l-1}\Delta r_{k-l-1}) + \frac{\Delta d_s}{d_s^3} \mid r_{k-l}^2 - r_{k-l-1}^2 \mid . \tag{23}$$

The interpretation of the symbols used in the formula is presented in fig. 22. It is shown in the context of a binaural sonar system. The form (23) indicates that the error can be reduced by

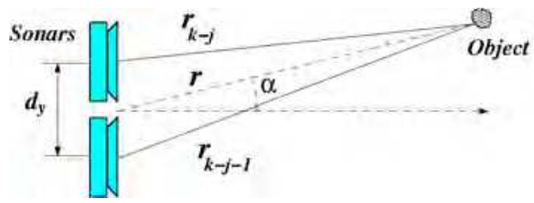

Fig. 22. The schema of sonars arrangement used to determine error values

enlarging the distance d_s between sonars. The chart in fig. 23 shows that the value of the error rapidly drops while d_s is enlarged up to about $9cm$. This conclusion isn't true with regard to a

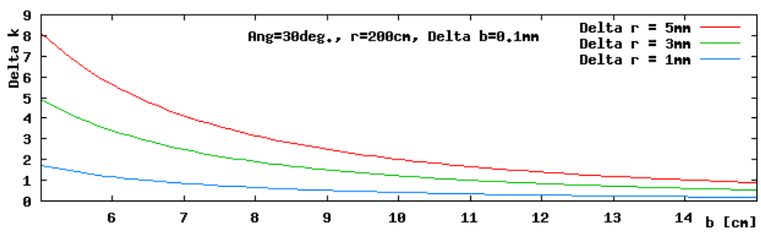

Fig. 23. The error estimation of k parameter as a function of the parameter b (distance between sonars). The error is estimated for an object placed at the distance $2m$ and the azimuth to the object is 30°

real distance $y = kd_s$ because

$$\Delta k d_s = \frac{1}{d_s}(r_{k-l}\Delta r_{k-l} + r_{k-l-1}\Delta r_{k-l-1}) + \frac{\Delta d_s}{d_s^2} \mid r_{k-l}^2 - r_{k-l-1}^2 \mid . \tag{24}$$

The chart in fig. 24 illustrates this relation. Unfortunately it isn't possible to increase the distance between sonars significantly. If it is enlarge too much, an object cannot be detected by all sonars. It is due to a restricted size of the emission angle. Another reason is that sonars have much lower sensitivity when a signal is received from a direction being far from their acoustic axis. For Polaroid transducers the distance between sonars up to $8cm$ seems to be reasonable. The error estimations presented in fig. 23 and fig. 24 are computed for a specific direction. But the conclusions are true for the whole range of the sonar sensibility. This is due to the fact that the error almost doesn't depend on the direction. The second component of the form (23) has

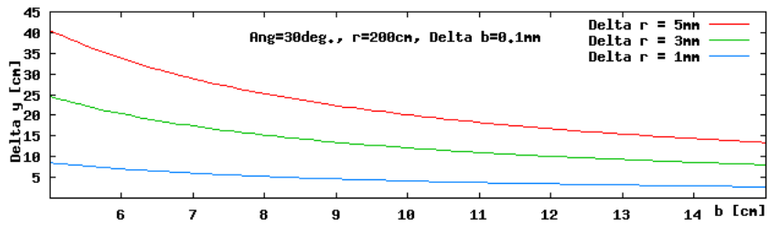

Fig. 24. The error estimation of the coordinate y of the object position. This error is a function of the parameter b (distance between sonars)

very small influence into the final value. This is also the reason that the error is almost linear in the sense of the distance to an object.
The same it can be said about the influence of the error Δr of distance measurement. Increasing the accuracy of the distance measurement it is possible to reduce the error of the parameter k. It can also be done by enlarging the distance d_s between sonars but unfortunately in a very limited range. Because it isn't possible to increase the distance between sonars without loosing detection of object located in the nearest robot surrounding. The error analyze presented in this section shows that it is possible if the accuracy of distance measurement is $1mm$ and the distance between sonars is $8cm$. In this way the condition $\Delta k \leq 1$ is guaranteed up to about $3m$ to an object.

6. Experiments

This section presents a sample of a few experiments. The obtained measurement data have been used for testing the presented approaches. The experiments checking the differentiation method have been performed using a binaural sonar system whose length of the baseline is $b = 13.6cm$. The same sonar arrangement was used for testing the triangulation method. The aforementioned system consists of Polaroid transducers 600–series model and the 6500 ranging modules. They were modified in the same way described in the section 2. The sonar system used in experiment isn't precise. Its measurement error is $2mm$. Therefore objects being the targets had to be placed enough close to the sonar system.
To test the method of objects differentiation presented in this chapter three objects were used i.e. a single plane, two planes arranged in a corner shape and others two planes arranged in an edge. They were placed at the distance about $0.5m$. The measurement were performed for three orientations. They were restricted to very narrow sector because echos were detected using the threshold method. Out of this sector the distance measurement is rapidly changed. It is due to attenuation of a received signal amplitude. Because the error of measurement was $2mm$, thus $\Delta C_e = 8mm$ and $\Delta C_w = \Delta C_c = 32000mm^2$. The computed values of C_e, C_w and

		edge			wall			corner		
	ΔC	$-3.7°$	$0°$	$3.7°$	$-3.7°$	$0°$	$3.7°$	$-3.7°$	$0°$	$3.7°$
C_e	8	**7**	**5**	**3**	24	24	20	-11	-16	-10
C_w	32000	-44503	-53583	-61575	**26180**	**26340**	**10436**	-117191	-139968	-115468
C_c	32000	102113	94313	85881	174076	173916	156604	**24945**	**4800**	**29908**

Table 1. The results of the object classification

C_c for all performed measurements are presented in tab. 1. They allow properly to classify all objects.
In the second part the previously obtained results of measurements have been used to determine the location of the objects. The computations have been performed for $\Delta r = 1.0625mm$ (it gives $b = 128\Delta r$), $d_r = 16\Delta r$, $n = 16$ and $m = 8$ (parameters meaning see (22) and fig. 21). Applying these parameters a look-up table has been constructed containing values of r and α in each cell. They represent the polar coordinates of the middle of the grid cell (see fig. 20b). Using the results of measurements the indexes of $\tilde{k}_y$ and $\tilde{k}_r$ have been computed. These indexes were used for r and $alpha$ values selection from the look-up tables. The procedure of this procedure has been described in subsectionsec-multi-sonar-system. The obtained results are presented in tab. 2. They are not very accurate due to measurements errors and errors

	edge			wall			corner		
	$-3.7°$	$0°$	$3.7°$	$-3.7°$	$0°$	$3.7°$	$-3.7°$	$0°$	$3.7°$
$\tilde{r}$ $[mm]$	515	510	510	520	515	520	515	535	535
$\tilde{\alpha}$ $[°]$	-2.9	-1.0	2.9	-3.0	1.0	4.8	-5.1	1.8	4.07

Table 2. The results of the objects localization

caused by discretization. But differences seems do be acceptable.

7. Summary

The approaches presented in this paper make possible to implement the methods using a simple micro-controller. It can be done because operations on integer numbers are only needed. For the method of object differentiation this feature is obtained by simplifying the form of the criterion. But the simplification doesn't mean lower precise in classification. For the object localization method the confinement to the integer number arithmetic is achieved by exploiting the discretization proposed in the paper. Unfortunately, it introduces additional source of errors. Considering the both methods the critical issue is the the error of TOF measurement. To be able to obtain a full implementation of the proposed method using low price hardware a proper echo detection method is needed. The easiest approach to this problem is a detection of exceeding a given threshold. But it is very sensitive to a signal amplitude and therefore introduce rather big errors. This disadvantage can be eliminated using an approach based on a correlation function. But it requires more computation power of the system and more complicated hardware. In this context the future work is concentrated on a method of the echo detection and the TOF measurement performance which should be able to combine simplicity of the threshold method and the accuracy of the methods based on the correlation function. Reaching satisfactory result it will be possible to build a low price smart sensor allowing to locate an object an identify some features of its surface shape. This seems to be a very good alternative solution comparing with traditional ultrasonic range-finders. Besides, it can be a very good complementary equipment to other set of sensors like laser range-finder, PSD sensors and vision systems.

8. References

Akbarally, H. & Kleeman, L. (1995). A sonar sensor for accurate 3d target localisation and classification. In: *Robotics and Automation, 1995. Proceedings., 1995 IEEE International Conference on*, volume 3, pages 3003–3008.

Angrisani, L. & Moriello, R. S. L. (2006). Estimating ultrasonic time-of-flight through quadrature demodulation. *IEEE Trans. on Instrumentation and Measurement*, 55(1):54 – 62.

Ayrulu, B.; Barshan, B., & Utete, S. (1997). Target identification with multiple logical sonars using evidential reasoning and simple majority voting. In: *Robotics and Automation, 1997. Proceedings., 1997 IEEE International Conference on*, volume 3, pages 2063–2068.

Brown, M. K. (1985). Feature extraction techniques for recognizing solid objects with an ultrasonic range sensors. *IEEE Journal of Robotics and Automation*.

Cheeke, J. D. N. (2002). *Fundamentals and Applications of Ultrasonic Waves*. CRC Press.

Egaña, A.; Seco, F., & Ceres, R. (2008). Processing of ultrasonic echo envelopes for object location with nearby receivers. *IEEE Trans. on Instrumentation and Measurement*, 57(12).

Heale, A. & Kleeman, L. (2001). Fast target classification using sonar. In: *Intelligent Robots and Systems, 2001. Proceedings. 2001 IEEE/RSJ International Conference on*, volume 3, pages 1446–1451 vol.3.

Jimenez, J.; Mazo, M.; Urena, J.; Hernandez, A.; Alvarez, F.; Garcia, J., & Santiso, E. (2005). Using pca in time-of-flight vectors for reflector recognition and 3-d localization. *Robotics, IEEE Transactions on*, 21(5):909–924.

Kleeman, L. (2004). Advanced sonar with velocity compensation. *Int. J. Robotics Res.*, 23.

Kleeman, L. & Kuc, R. (1995). Mobile robot sonar for target localization and classification. *Int. J. Robotics Res.*, 14(4):295 – 318.

Kreczmer, B. (1998). Path planning system for car-like robot. In: *Proc. 1998 IEEE Int. Conf. Robot. Automat.*, volume 1, pages 40 – 45.

Kreczmer, B. (2006). 3d object localization and distinguishing using triangular-shaped ultrasonic system. In: *Proc. 12th IEEE Int. Conf. MMAR 2006*, pages 931 – 936.

Kuc, R. (2001). Pseudoamplitude scan sonar maps. *IEEE Trans. Robot. Automat.*, 17(5):787 – 770.

Kuc, R. (2007). Neuromorphic processing of moving sonar data for estimating passing range. *IEEE Sensors Journal*, 7(5):851 – 859.

Kuc, R. & Siegel, M. W. (1987). Physically-based simulation model for acoustic sensor robot navigation. *IEEE Trans. on Pattern Anal. and Mach. Intell.*, 9:766 – 778.

Leonard, J. J. & Durrant-Whyte, H. F. (1991). Mobile robot localization by tracking geometric beacons. *IEEE Trans. Robot. Automat.*, 7(3):376–382.

Li, H. M. & Kleeman, L. (1995). A low sample rate 3d sonar sensor for mobile robots. In: *Robotics and Automation, 1995. Proceedings., 1995 IEEE International Confe rence on*, volume 3, pages 3015–3020.

Ochoa, A.; Urena, J.; Hernandez, A.; Mazo, M.; Jimenez, J., & Perez, M. (2009). Ultrasonic multitransducer system for classification and 3-D location of reflectors based on pca. *Instrumentation and Measurement, IEEE Transactions on*, 58(9):3031–3041.

Peremans, H.; Audenaert, K., & Campenhout, J. M. V. (1993). A high-resolution sensor based on tri-aural perception. *IEEE Trans. Robot. Automat.*, 9(1):36 – 48.

Schillebeeckx, F.; Reijniers, J., & Peremans, H. (2008). Probabilistic spectrum based azimuth estimation with a binaural robotic bat head. In: *4th Inter. Conf. on Autonomic and Autonomous Systems*, pages 142 – 147.

IntechOpen

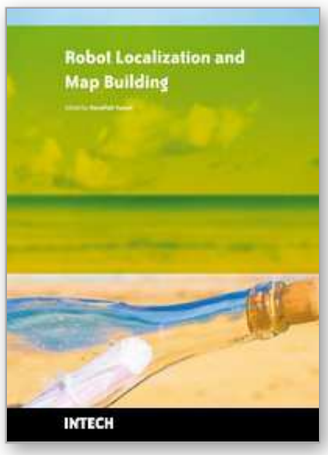

Robot Localization and Map Building

Edited by Hanafiah Yussof

ISBN 978-953-7619-83-1
Hard cover, 578 pages
Publisher InTech
Published online 01, March, 2010
Published in print edition March, 2010

Localization and mapping are the essence of successful navigation in mobile platform technology. Localization is a fundamental task in order to achieve high levels of autonomy in robot navigation and robustness in vehicle positioning. Robot localization and mapping is commonly related to cartography, combining science, technique and computation to build a trajectory map that reality can be modelled in ways that communicate spatial information effectively. This book describes comprehensive introduction, theories and applications related to localization, positioning and map building in mobile robot and autonomous vehicle platforms. It is organized in twenty seven chapters. Each chapter is rich with different degrees of details and approaches, supported by unique and actual resources that make it possible for readers to explore and learn the up to date knowledge in robot navigation technology. Understanding the theory and principles described in this book requires a multidisciplinary background of robotics, nonlinear system, sensor network, network engineering, computer science, physics, etc.

InTech Europe
University Campus STeP Ri
Slavka Krautzeka 83/A
51000 Rijeka, Croatia
Phone: +385 (51) 770 447
Fax: +385 (51) 686 166
www.intechopen.com

InTech China
Unit 405, Office Block, Hotel Equatorial Shanghai
No.65, Yan An Road (West), Shanghai, 200040, China
中国上海市延安西路65号上海国际贵都大饭店办公楼405单元
Phone: +86-21-62489820
Fax: +86-21-62489821

IntechOpen